MO Studies on Palladium(0)-Derivatives of Buckminsterfullerene (C_{60})

Kee Hag Lee*, Han Myoung Lee, and Wang Ro Lee

Department of Chemistry, WonKwang University, Iri 570-749, Korea
Received January 6, 1995

The electronic structures of $(H_3P)_2Pd(\eta^2\text{-}C_2H_4)$ and $(H_3P)_2Pd(\eta^2\text{-}C_{60})$ are calculated by using the EHMO method with modified EH parameters. Our results for Pd-derivatives show that the carbon-carbon double bonds of C_{60} and ethene react like those of electron-poor arenes and alkenes, which are analogous with the previous results for Pt-derivatives. In Pd-C_{60} derivative the electronic charge transferred from filled palladium *d*-orbital is localized at the two carbon atoms of the double bond to which Pd-ligand is attached.

Introduction

The interaction of fullerenes with molecules has been of fundamental interest, so several papers showed the chemical reactivity between metal (Os, Pt, Ir) complexes and C_{60} *via* solution chemistry forming metal-C_{60} bonds. Hawkins *et al.*[1] have synthesized a one-to-one C_{60}-osmium tetroxide adduct, $C_{60}(OsO_4)$(4-tert-butylpyridine)$_2$. Balch *et al.*[2] have shown that addition of an equimolar amount of a purple solution of C_{60} in benzene to a yellow benzene solution of $Ir(CO)Cl(PPh_3)_2$ immediately forms a deep brown solution from which black-brown crystals of $(\eta^2\text{-}C_{60})Ir(CO)Cl(PPh_3)_2\cdot 5C_6H_6$ precipitate. It has been reported that, for the platinum complex $[(C_6H_5)_3P]_2Pt(\eta^2\text{-}C_{60})$, the reactivity of C_{60} is not like that of relatively electron-rich planar aromatic molecules such as benzene, that is, the carbon-carbon double bonds of C_{60} behave chemically like those of very electron-deficient arenes and alkenes.[3] In terms of the platinum coordination sphere, it was found that this C_{60} complex formed at the junction of two fused 6-membered rings (6-MRs) in C_{60} closely resembles the structures seen for another platinum alkene complex, $[(C_6H_5)_3P]_2Pt(\eta^2$-ethylene). Also, using NMR spectra and X-ray crystalographic results of the hexa-substituted platinum derivative $\{[(C_6H_5)_3P]_2Pt\}_6C_{60}$, Fagan *et al.*[4] have shown that the molecule has a multiply-substituted buckminsterfullerene with an octahedral array of platinum atoms. And they have investigated the electrochemical properties of the complexes $(Ph_3P)_2Pt(\eta^2\text{-}C_{60})$, $(Et_3P)_2M(\eta^2\text{-}C_{60})$, $[(Et_3P)_2M]_6C_{60}$ (M=Ni, Pd, Pt; Et=ethyl, Ph=phenyl), and $[(Et_3P)_2Pt]_nC_{60}$ (n=2-4). Bashilov *et al.*[5] have shown the synthesis and molecular structure of the Palladium(0)-fullerene derivative $(\eta^2\text{-}C_{60})Pd(PPh_3)_2$. Their structural studies for metal complexation suggest that the bonds between two fused six-membered rings in C_{60} are the most reactive, these bonds being shorter and having the most double bond character. The fact that low-valent metal centers like Ir(I) and Pt(0) add to the carbon atoms at 6-6 membered ring fusions in C_{60} was consistent with the predictions of bond localization energy calculations.[6]

Ab initio results[7] for $(H_3P)_2Pt(\eta^2\text{-}C_{60})$ have shown that the charge transfer from Pt fragment is 0.926 and the binding energy between fragments ($Pt(PH_3)_2$ and C_{60}) is 0.95 eV. Fann *et al.*[8] have used the EHMO method to calculate the electronic correlation between C_{60} and the bunnyballs (Os-C_{60}, Ru-C_{60} and Mn-C_{60} complexes). The energy level correlation of C_{60} in their EH work is different from those of 3D-Hückel,[9]

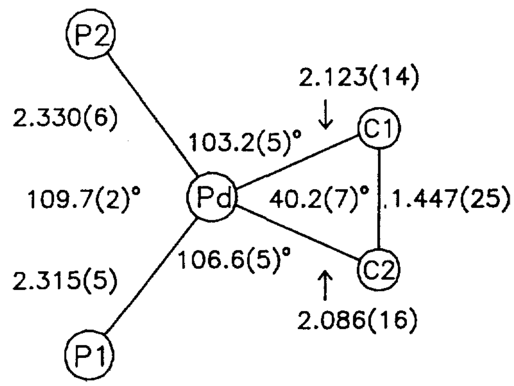

Figure 1. Geometry of the Pd coordination spheres in $(H_3P)_2Pd(\eta^2\text{-}C_{60})$.[7]

DV-Xα,[10] and CNDO/S.[11] Lee *et al.*[13] have used the EHMO method to calculate the electron energy level correlation of C_{60} and C_{60}-Pt derivative. Results with modified parameter set in our previous work reasonably represent *ab initio* result of Morokuma and Koga.[7]

Model and Calculation

We have calculated the electronic structure and properties of $(H_3P)_2Pd(\eta^2\text{-}C_{60})$ and $(H_3P)_2Pd(\eta^2\text{-}C_2H_4)$ using the EHMO method. The previous parameter set (parameter set **1**) and the modified parameter set (parameter set **2**) for carbon and the Hückel constant are used. The parameters of the other atoms (H, P and Pd) in these complexes are not changed in this work (see APPENDIX).[12] The results are compared with those for the Pt-derivatives. For the sake of simplifying the calculations, we substitute hydrogens for the phenyl groups of Pd-ligands. The distances and the bond angles around palladium in Pd-C_{60} derivative are obtained from reference [7] and shown in Figure 1, and those in Pd-C_2H_4 derivative are taken from those of Pt-C_2H_4 derivative.[3] But as far as we know both experimental and theoretical studies of the complex formed by addition of Pd-ligand to a junction of 5- and 6-MRs of C_{60} were not reported. The difference of structure between two types of Pd-C_{60} complex, and the variation of bond lengths around the fusion of 5-6MRs of C_{60} affected by Pd-ligand are not considered.

The fragment molecular orbital (FMO) calculations for

Table 1. Results from EH-FMO Calculations for $(H_3P)_2Pd(\eta^2-C_2H_4)$ and $(H_3P)_2Pd(\eta^2-C_{60})$ with Each Parameter Set

	Parameter sets	HOMO-LUMO gap (eV) $(H_3P)_2Pd$	R	$(H_3P)_2Pd(\eta^2-R)$	Charge of $Pd(PH_3)_2$	Charge variation of Pd, Δq	Relative BE (eV)^a
$(H_3P)_2Pd(\eta^2-C_2H_4)$	1	6.02	3.98	4.04	0.395	0.349	0.00
	2	6.23	4.94	4.27	0.624	0.546	0.00
$(H_3P)_2Pd(\eta^2-C_{60})$,	1	6.05	1.46	1.36	0.427	0.369	0.07
(at 6-6MR)	2	6.20	1.95	0.15	1.113	0.983	1.09
$(H_3P)_2Pd(\eta^2-C_{60})$,	1	6.05	1.60	0.96	0.305	0.295	−0.42
(at 5-6MR)	2	6.20	2.06	0.33	1.741	1.587	−0.45

R = C_2H_4 or C_{60}; Δq = Charge of Pd in $(H_3P)_2Pd(\eta^2-R)$-Charge of Pd in $Pd(PH_3)_2$; a = (the sum of Energies of $(H_3P)_2Pd$ and R − Energy of Complex) − BE of $(H_3P)_2Pd(\eta^2-C_2H_4)$

Table 2. The Net Charges of The Carbon Atoms of C_2H_4 and C_{60} Attached by Pd-ligand

Complex	Parameter sets	Net charge of carbons: Fragment C1	Fragment C2	Complex C1	Complex C2
$(H_3P)_2Pd(\eta^2-C_2H_4)$	1	−0.08	−0.08	−0.24	−0.25
	2	−0.18	−0.18	−0.47	−0.47
$(H_3P)_2Pd(\eta^2-C_{60})$,	1	−0.08	−0.08	−0.12	−0.12
(at 6-6MR)	2	−0.05	−0.05	−0.20	−0.21
$(H_3P)_2Pd(\eta^2-C_{60})$,	1	0.00	0.00	0.03	0.03
(at 5-6MR)	2	0.00	0.00	−0.04	−0.06

$(H_3P)_2Pd$-(η^2-C_{60}) with fragments, η^2-C_{60} and $Pd(PH_3)_2$, and for $(H_3P)_2Pd(\eta^2-C_2H_4)$ with fragments, $\eta^2-C_2H_4$ and $Pd(PH_3)_2$ give orbital interaction diagrams as shown in Figures 2, 3 and 4.

Results and Discussion

Table 1 shows the energy differences between the highest occupied molecular orbital (HOMO) and the lowest unoccupied molecular orbital (LUMO) in complexes and each fragment, the charges of $Pd(PH_3)_2$ fragment in each complex, the charge variations of Pd between Pd-ligand and Pd-derivatives, and the relative binding energies (BE) of each complex from the two fragments.

The relative BE of parameter set **2** is reasonable, not absolute. Here the BE means the negative formation energy of complex from fragments. $(H_3P)_2Pd(\eta^2-C_{60})$ (complex type **1**) formed by addition of Pd-ligand to a junction of 6-6MRs of C_{60} is the most stable. The relative BE of the cases in parameter set **2** are higher than those in parameter set **1**. And the relative BE for $(H_3P)_2Pd(\eta^2-C_2H_4)$ is higher than that for Pd-C_{60} derivative (complex type 2) formed with Pd-ligand attaching to a junction of 5- and 6-MRs of C_{60}. These results are almost the same as our earlier results of Pt-derivatives.[13] The exception is that the absolute value of complex formation energy of Pd-ethylene derivative with parameter set **1** is smaller than that of Pd-C_{60} complex type **1**, but vice versa in the results of Pt-complexes.

The electron acceptivity of C_2H_4 or C_{60} is stronger in parameter set **2** than set **1**. In parameter set **2** case, the electron acceptance of C_{60} in Pd-C_{60} derivatives is stronger in type **2** than type **1**. The electron acceptivity in Pd-derivatives is stronger in C_{60} than ethylene. But in parameter set **1** case, the electron acceptivity of C_{60} in Pd-C_{60} complex is stronger in type **1** than type **2**. In Pd-derivatives, the strength of the electron acceptance of ethylene is between those of C_{60} in type **1** and type **2**.

Table 2 shows the net charges of the carbon atoms of C_2H_4 and C_{60}, which are the carbon sites attached by Pd-ligand in fragments and complex. In the results of EH calculations for Pd-C_2H_4 with each parameter set, the net charges of the carbon atoms at the interacting carbons become larger in complex than in fragment, and the charges of the interacting carbons are larger for parameter set **2** than for set **1**. In Pd-C_{60} complex type **1**, the electron charges of the two carbon sites attached by Pd-ligand are larger in parameter set **2** than set 1. The electron at the sites in the double bond of C_{60} is more localized in Pd-C_{60} than that in Pt-C_{60}. But in the case of Pd-C_{60} complex type **2**, the electron charges of the two carbon atoms are small, in comparison with the electron acceptivity of C_{60} from Pd-ligand (Table 1).

The HOMO-LUMO energy gap for the fragment C_{60} and C_2H_4 is larger in parameter set **2** than in set **1**. As shown in Figures 2, 3 and 4, the orbital interaction of the HOMO of Pd-ligand and the LUMO of C_{60} (or C_2H_4) is larger in parameter set **2** than in set **1**. In both of two Pd-C_{60} type complexes the energy gap is smaller than fragment C_{60}.

At first, Figure 2 shows the orbital interaction diagrams by the calculations of $(H_3P)_2Pd(\eta^2-C_2H_4)$ in which phosphorus, palladium, and carbon atoms are closely associated with C_{2v} point group symmetry. Figure 2(a) is the results with the parameter set **1**. The fragment orbitals from the HOMO to 5th HOMO of Pd-ligand have strong nonbonding metal orbital character. There is an interaction between the LUMO (π^*) of the ethylene-fragment and the HOMO orbital of Pd-fragment, in which the HOMO of d_{xz} character is stabilized by a symmetrically matched π^* orbital as electron acceptor. This interaction forms the LUMO and the 2nd HOMO of this complex. But the interaction between the 5th HOMO of d_{z^2} character of Pd-fragment and π-orbital of ethylene has little of effect on the stabilization of complex. Figure 2(b) shows the orbital interaction diagrams with the parameter set **2**. As in the Figure 2(a), the HOMO of Pd-fragment interacts with

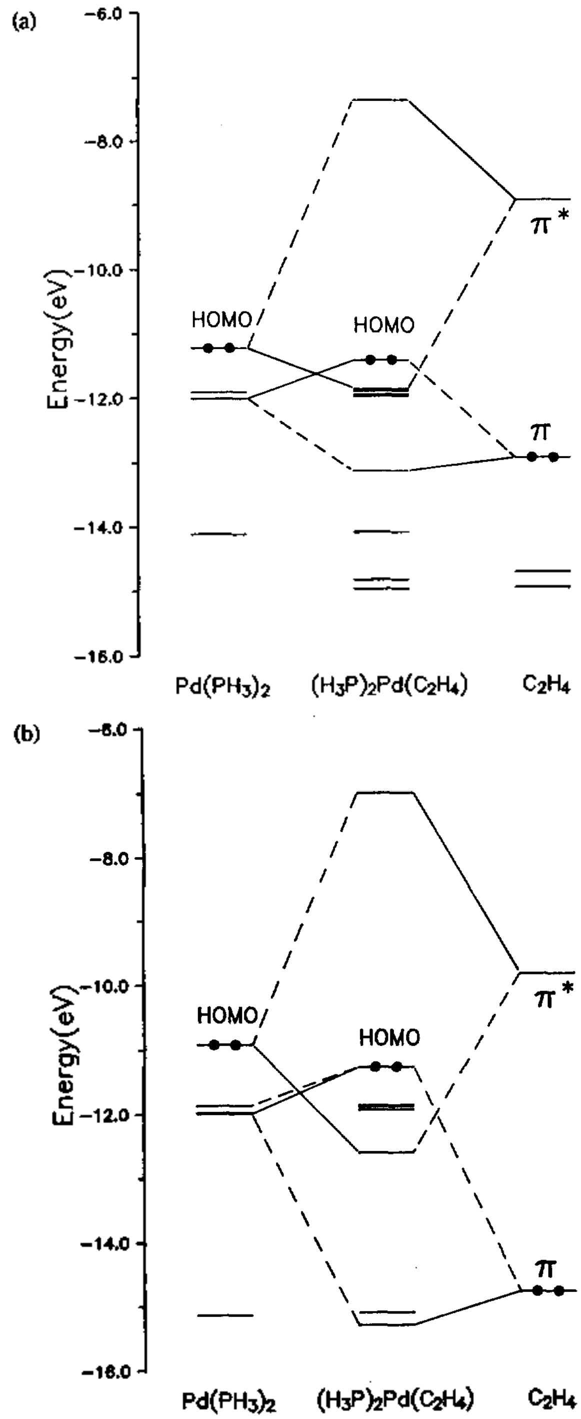

Figure 2. Molecular orbital interaction diagrams of $(H_3P)_2Pd(\eta^2\text{-}C_2H_4)$, (a) with the (previous) parameter set **1** and (b) with the (modified) parameter set **2**.

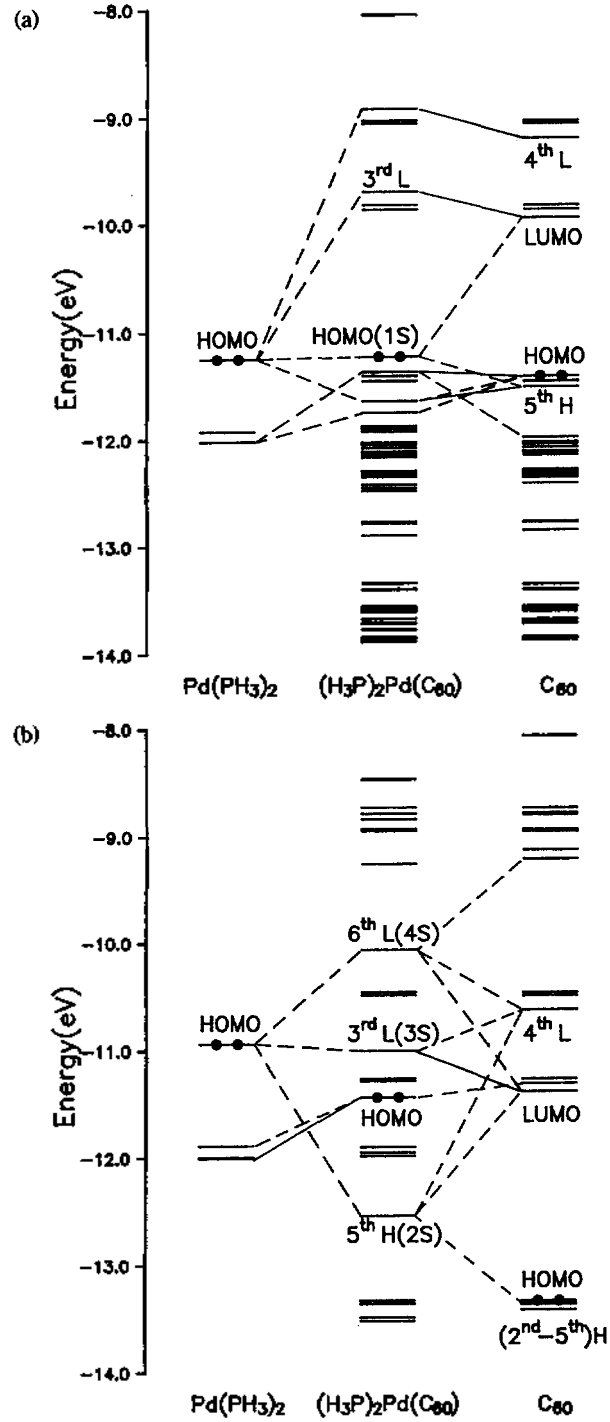

Figure 3. Molecular orbital interaction diagrams of $(H_3P)_2Pd(\eta^2\text{-}C_{60})$ formed by addition of Pd-ligand to a junction of two 6-MRs of C_{60}, (a) with the (previous) parameter set **1** and (b) with the (modified) parameter set **2**. Here numbered H(L) means n^{th} HOMO (LUMO), and (numbered S) means the MO energy level of Scheme number.

π^* (LUMO) of ethylene, forms a stabilized molecular orbital (5^{th} HOMO of complex), and transfers electron to ethylene analogous with Pt-C_2H_4 derivative.[13] Also, there is an interaction between the 5^{th} HOMO of Pd-ligand and π-orbital of ethylene fragment. But the energy difference of the HOMO of Pd-fragment and the LUMO of ethylene in Figure 2(b) is smaller than that in Figure 2(a), and then the interaction and the electron acceptance of ethylene in Figure 2(b) is larger than in Figure 2(a).

The molecular orbital interaction diagrams by the EHMO calculations for Pd-C_{60} complex type **1**, $(H_3P)_2Pd(\eta^2\text{-}C_{60})$, are

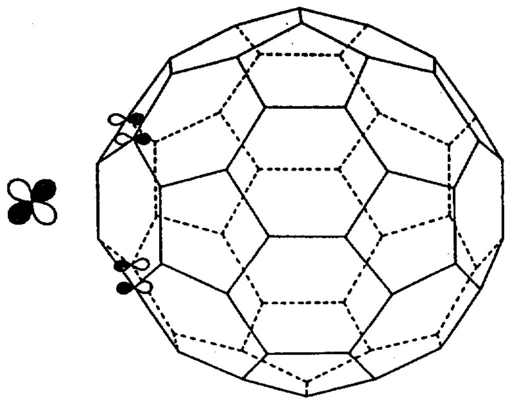

Scheme 1.

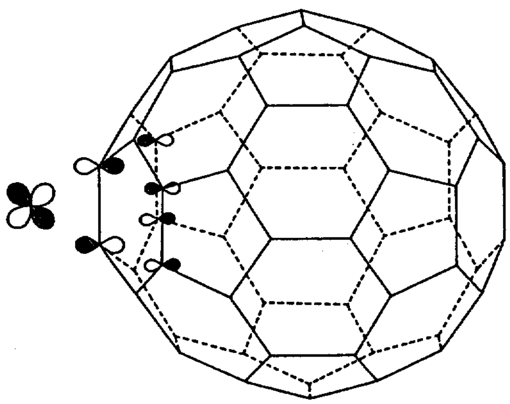

Scheme 2.

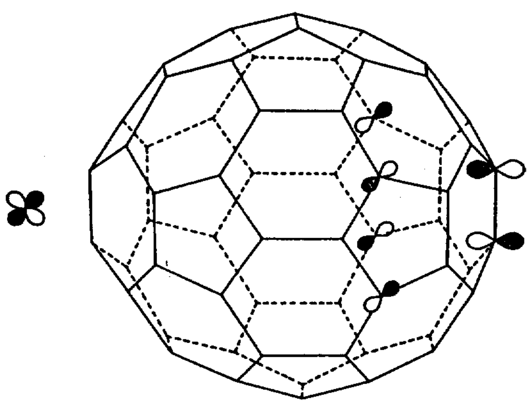

Scheme 3.

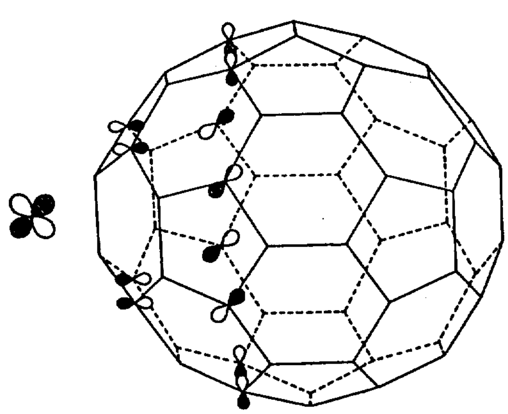

Scheme 4.

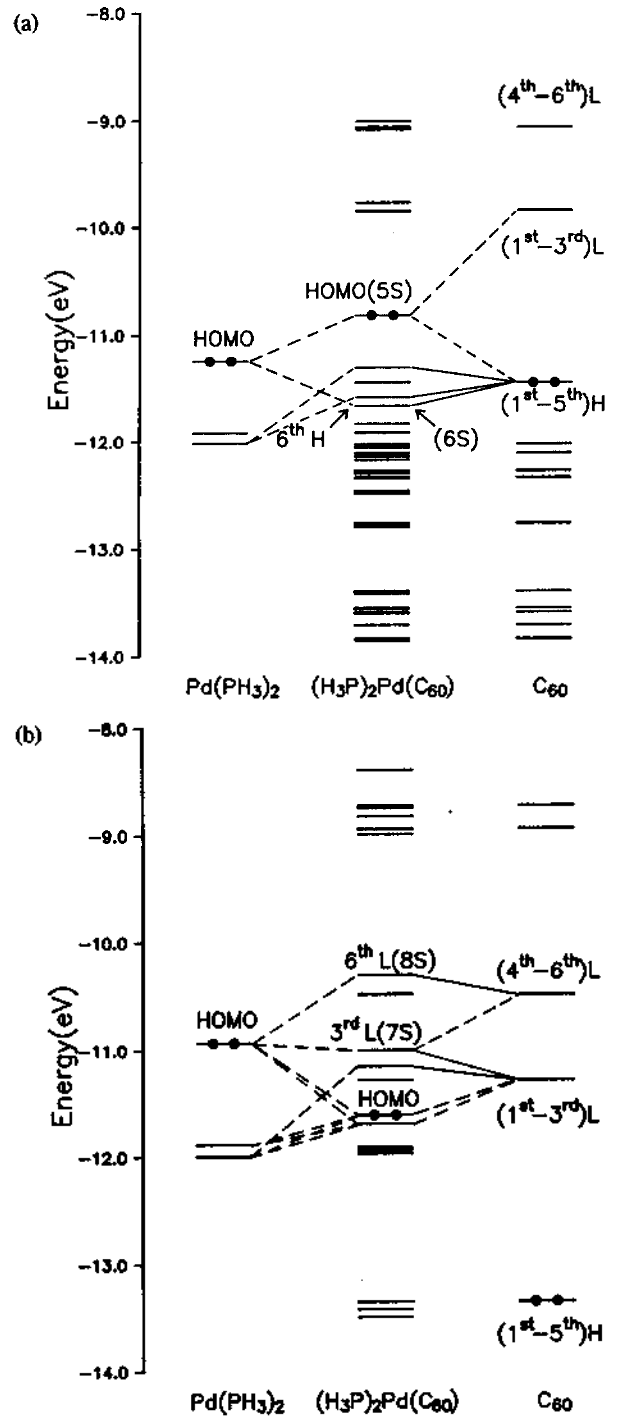

Figure 4. Molecular orbital interaction diagrams of $(H_3P)_2Pd$-(η^2-C_{60}) formed by addition of Pd-ligand to a junction of 5- and 6-MRs of C_{60}, (a) with the (previous) parameter set 1 and (b) with the (modified) parameter set 2. Here numbered H(L) means n^{th} HOMO (LUMO), and (numbered S) means the MO energy level of Scheme number.

exhibited in Figure 3. The results with the parameter set 1 are shown in Figure 3(a), the results with set 2 are in Figure 3(b). From calculations of $(H_3P)_2Pd(\eta^2$-$C_{60})$ with parameter set 1, the interactions between the HOMO of d_{xz} character of Pd-fragment and both the LUMO and 3^{rd} HOMO

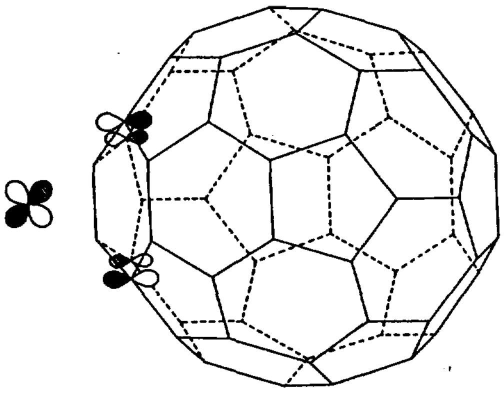

Scheme 5.

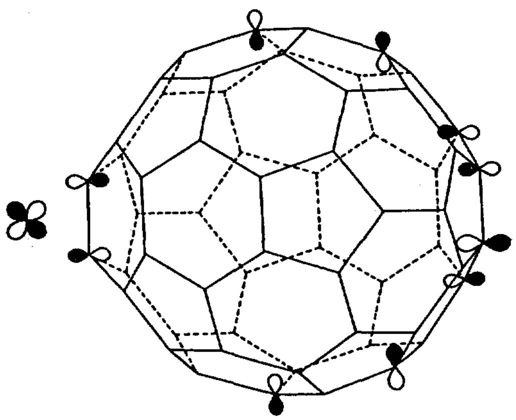

Scheme 6.

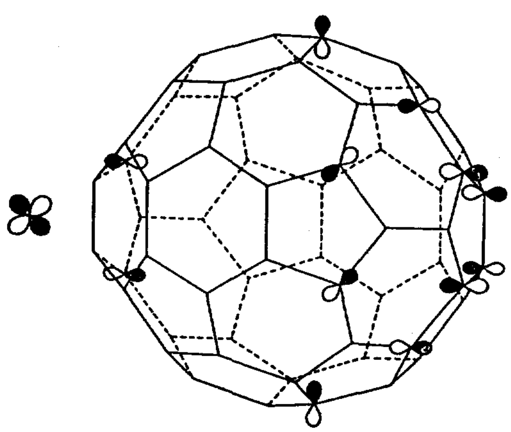

Scheme 7.

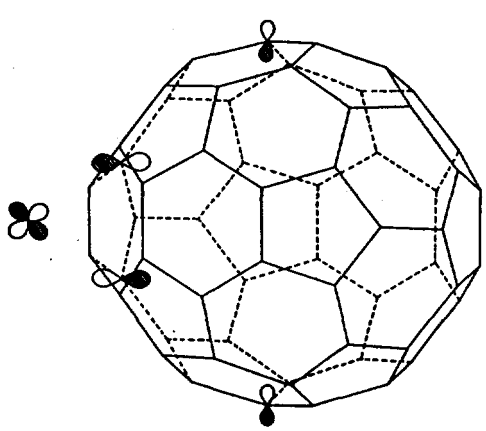

Scheme 8.

of C_{60} produce three molecular orbitals (one bonding and two antibonding) of Pd-derivative of this type **1**. The 3rd LUMO of Pd-complex comes mainly from nonbonding MO of C_{60} fragment. But the HOMO of Pd-derivative has antibonding character as shown in Scheme 1. In Figure 3(b), which is the result with parameter set 2, it is different from the $(H_3P)_2Pd(\eta^2\text{-}C_2H_4)$ in that the HOMO of Pd-ligand has higher energy than the LUMO of C_{60}-fragment. But the energy difference between the HOMO of d_{π} character of Pd-fragment and the LUMO of C_{60} is much smaller than that in the case with parameter set 1. The fragment HOMO of Pd-ligand is stabilized by both the LUMO and the 4th LUMO of C_{60} fragment. These fragment orbitals make one bonding molecular orbital (the 5th HOMO) and two antibonding molecular orbitals (the 3rd and the 6th LUMOs of Pd-derivative). Scheme 2 shows the 5th HOMO of Pd-derivative. The LUMO and the 4th LUMO of C_{60} fragment are hybridized to form the 3rd LUMO of this type complex with the HOMO of Pd-fragment. The orbital lobes in the opposite of the attached position of C_{60} are larger in the 3rd LUMO of Pd-complex as shown in Scheme 3. Scheme 4 of the 6th LUMO of this complex shows antibonding character. But the orbital coefficients of the attached carbon atoms of C_{60} is very small. In the result (Figure 3(a)) with parameter set 1, the 3rd LUMO is alike with Scheme 3 and the HOMO alike with Scheme 4. In this way electron is transferred to C_{60}-fragment from Pd-ligand. These interactions between Pd-ligand and C_{60} in the diagrams of Figure 3 are analogous to those[13] of Pt-ligand and C_{60}.

Figure 4 shows the results from the calculations for Pd-C_{60} complex of type **2**. Figure 4(a) is the results with parameter set 1. The HOMO of Pd-fragment and the HOMO of C_{60} fragment interact to make the unstable antibonding MO (HOMO) and the bonding MO (6th HOMO) of Pd-C_{60} derivative. Schemes 5 and 6 represent the HOMO and 6th HOMO of Pd-complex of this type. In Scheme 5 of antibonding character the orbital lobes of the next ones to the attached carbon atoms of C_{60} are considerably large. In Scheme 6 of the 6th HOMO of Pd-derivative the interaction analogy to the Scheme 2 of Pd-complex type **1** appears, and the orbital lobes of the opposite ones of the attached sites of C_{60} are appropriately large. Figure 4(b) as the results of parameter set 2 shows interactions between nonbonding metal orbitals of $Pd(PH_3)_2$-fragment and unoccupied fragment orbitals of C_{60}. The 6th and 3rd LUMOs of this Pd-C_{60} complex are displayed in Schemes 7 and 8 which are antibonding, but the orbital coefficients of the carbon atoms bonded to the Pd-ligand are disappeared. The HOMO of Pd-ligand is stabilized to make the HOMO and unoccupied MOs of this type **2** of Pd-C_{60} derivative. This fragment orbital interaction diagram is more a little complicate than that of Pt-C_{60} complex.

Conclusion

From EH-FMO calculations using the modified parameter, the HOMO of Pd-fragment interacts with electron-empty fragment orbitals of C_{60} or ethylene. The HOMO is stabilized by transferring its electrons to the empty orbitals of C_{60} or C_2H_4. Our results show that carbon-carbon double bonds of C_{60} and C_2H_4 react like those of electron-poor arenes and alkenes, and also that C_{60} is more electron-susceptible than

APPENDIX; Parameters used in EHMO Calculation

Atom	s			p			d					
	n	−IP	ζ	n	−IP	ζ	n	−IP	ζ_1	ζ_2	c_1	c_2
H	1	13.6	1.30									
C(set 1)	2	21.4	1.625	2	11.4	1.625						
C(set 2)	2	21.4	1.92	2	12.67	1.92						
P	3	18.6	1.75	3	14.0	1.30						
Pd	5	7.32	2.19	5	3.75	2.152	4	12.02	5.983	2.613	0.5535	0.6701

Here, the Hückel constant, K is 1.75 and 2.35 in parameter set **1** and **2**, respectively.

C_2H_4. In Pd-C_{60} derivative type **1**, two carbon sites of the double bond of C_{60} localize electrons transferred from Pd-ligand.

Acknowledgment. This research was supported through KOSEF grant 94-080011013. We are grateful to Professor Y. Lee, KAIST, for his comment.

References

1. Hawkins, J. M.; Meyer, A.; Lewis, T. A.; Stefan Loren; Hollander, F. J. *Science* **1991**, *252*, 312.
2. Balch, A. L.; Catalano, V. J.; Lee, J. W. *Inorg. Chem.* **1991**, *30*, 3980.
3. Fagan, P. J.; Calabrese, J. C.; Malone, B. *Science* **1991**, *252*, 1160.
4. Fagan, P. J.; Calabrese, J. C.; Malone, B. *J. Am. Chem. Soc.* **1991**, *113*, 9408.
5. Bashilov, V. V.; Petrovskii, P. V.; Sokslov, V. I.; Lindeman, S. V.; Guzey, I. A.; Struchkov, Y. T. *Organometallics* **1993**, *12*, 991.
6. Amié, D.; Trinajstiĉ, N. *J. Chem. Soc., Perkin Trans.* **1990**, *2*, 1595.
7. Koga, N.; Morokuma, K. *Chem. Phys. Lett.* **1993**, *202*, 330.
8. Fann, Y. C.; Singh, D.; Jansen, S. A. *J. Phys. Chem.* **1992**, *96*, 5817.
9. Haddon, R. C.; Brus, E. L.; Raghavachari, K. *Chem. Phys. Lett.* **1986**, *125*, 459.
10. Hale, P. D. *J. Am. Chem. Soc.* **1986**, *108*, 6087.
11. Leach, S.; Vervloet, M.; Despres, A.; Breheret, E.; Hare, J. P.; Dennis, T. J.; Kroto, H. W.; Taylor, R.; Walton, D. R. M. *Chem. Phys.* **1992**, *160*, 451.
12. (a) Hoffmann, R. *J. Chem. Phys.* **1963**, *39*, 1397. (b) Summerville, R. H.; Hoffmann, R. *J. Am. Chem. Soc.* **1976**, *97*, 7240. (c) Tatsumi, K.; Hoffmann, R.; Yamamoto, A., Stille, J. K. *Bull. Chem. Soc. Jpn.* **1981**, *54*, 1857.
13. Lee, K. H.; Lee, H. M. and Lee, W. R. *Bull. Kor. Chem. Soc.* **1995**, *16*, 226.

Electrical Properties of TiO_{2-x} Thin Films by Thermal Oxidation

Yong-Kook Choi*, Q-Won Choi†, Ki-Hyung Chjo, and Seung-Won Jeon

Department of Chemistry, Chonnam National University, Kwangju 500-757, Korea

†Department of Chemistry, Seoul National University, Seoul 151-742, Korea

Received February 23, 1995

The electrical properties of the TiO_{2-x} thin films prepared by thermal oxidation from titanium sheets have been studied. The films by water vapor oxidation are oxidized more homogeneously than those by air oxidation. The electrical contact to measure the electrical conductivity of the TiO_{2-x} electrodes is improved when the electrode surface is plated with silver. The hysterisis of the electrical conductivity curves is improved by applying alternating current rather than direct current on both sides of the electrode. The observed energy gap, E_d are 0.05-0.16 and 0.11-0.76 eV, respectively, at low and high temperatures region. These values of the TiO_{2-x} electrode prepared by water vapor oxidation are similar to those of single crystal TiO_2. The values of donor concentration, N_D, are observed about 10^{15}-10^{19} and 10^{17}-10^{21} cm^{-3}, respectively, at low and high temperatures region. These values obtained at high temperature region are consistent with the values obtained from Mott-Schottky plot.

Introduction

The electrical and photo-electrochemical properties of semiconductor electrodes have been studied for the purpose of changing the solar energy into an electrochemical energy.[1-35] Many semiconductor materials have been used as